Correlated Insulated Phase Suggests Bond Order between Band and Mott Insulators in Two Dimensions

S. S. Kancharla[1] and E. Dagotto[1,2]

[1]*Materials Science and Technology Division, Oak Ridge National Laboratory, Oak Ridge, Tennessee 32831, USA*
[2]*Department of Physics and Astronomy, University of Tennessee, Knoxville, Tennessee 37996, USA*

(Received 21 July 2006; published 5 January 2007)

We investigate the ground state phase diagram of the half-filled repulsive Hubbard model in two dimensions in the presence of a staggered potential Δ, the so-called ionic Hubbard model, using cluster dynamical mean-field theory. We find that for large Coulomb repulsion, $U \gg \Delta$, the system is a Mott insulator (MI). For weak to intermediate values of Δ, on decreasing U, the Mott gap closes at a critical value $U_{c1}(\Delta)$ beyond which a correlated insulating phase with possible bond order is found. Further, this phase undergoes a first-order transition to a band insulator (BI) at $U_{c2}(\Delta)$ with a finite charge gap at the transition. For large Δ, there is a direct first-order transition from a MI to a BI with a single metallic point at the phase boundary.

DOI: 10.1103/PhysRevLett.98.016402 PACS numbers: 71.10.Fd, 71.10.Hf, 71.27.+a

The Mott metal-insulator transition is a paradigmatic problem in condensed matter physics that has been realized in a broad set of experiments, ranging from the high temperature superconductors to recently observed phenomena involving cold atoms trapped in optical lattices. Mott insulators (MIs) are characterized by a density of one electron per unit cell and strong Coulomb interactions that often lead to symmetry breaking via antiferromagnetic (AF) order. In contrast, charge localization in band insulators (BIs) occurs when the number of electrons per unit cell is even, so that the bands are either full or empty. These two types of insulators can be realized within a single system, the ionic Hubbard model (IHM) at half filling, by tuning the strength of Coulomb interaction. The BI-MI quantum phase transition in the IHM has been well studied in the limit of either one [1–4] or infinite dimensions [5], but significant uncertainties remain in the phase diagram. Originally suggested to describe charge-transfer organic salts [6], there has been renewed interest in the model due to potential applications to ferroelectric perovskites [7]. Confinement of Fermionic atoms in an optical lattice to realize the ionic Hubbard model is also conceivable in the future, because recent experimental progress has allowed for Fermionic atoms to be cooled well below the degeneracy temperature [8].

Our objective in this Letter is to obtain the ground state phase diagram of the IHM at half filling in two dimensions using cluster dynamical mean-field theory (CDMFT) [9]. The IHM is realized on a bipartite lattice by the assignment of an alternating chemical potential ($\pm \Delta$) for each sublattice on top of the regular Hubbard model. The Hamiltonian can be written as

$$H = -t \sum_{i \in A j \in B} [c^{\dagger}_{i\sigma} c_{j\sigma} + \text{H.c.}] + U \sum_i n_{i\downarrow} n_{i\uparrow} + \Delta \sum_{i \in A} n_i - \Delta \sum_{i \in B} n_i - \mu \sum_i n_i. \quad (1)$$

Here, t and U denote the hopping amplitude between nearest-neighbor sites and the on-site Coulomb repulsion, respectively. $+\Delta(-\Delta)$ denotes the local potential energy for the $A(B)$ sublattice. We are interested in the case where the combined density of A and B sublattices is 1 and so we set the chemical potential, μ, to $U/2$. In the atomic limit ($t = 0$) and for $U/2 < \Delta$, the ground state has two electrons on the B sublattice and none on the A sublattice, resulting in charge density wave (CDW) order with a band gap of $\Delta - U/2$. In the opposite limit where $U/2 > \Delta$, each site is occupied by one electron and a MI is formed with a gap U. Therefore, in the atomic limit at exactly $U_c = 2\Delta$ the system is gapless [1–4]. This transition from a BI to a MI is likely to persist when $t \neq 0$, but nontrivial charge fluctuations in the intermediate to strong coupling regime ($U \sim 2\Delta$) render static mean-field and perturbative treatments of the transition invalid.

Bosonization calculations for the IHM in one dimension [4], valid in the weak coupling regime ($\Delta \ll U \ll t$), find a transition from a BI to a bond-ordered insulator at $U = U_c$, where the charge gap vanishes. The bond-ordered phase is characterized by finite charge and spin gaps. Increasing U further, the spin gap vanishes at $U = U_s$ in a Kosterlitz-Thouless–type transition leading to a MI. Numerical studies for long chains using the density matrix renormalization group (DMRG) [2,3] in the strong coupling regime find that the charge gap remains finite at the transition point U_c to the bond-ordered phase, although the optical gap does vanish. The DMRG is unable to identify a second transition point towards a MI because extrapolation to large system sizes in the critical region is a challenge to numerical methods.

Our key findings for the IHM in two dimensions are the following. A nonzero staggered chemical potential induces CDW order over the entire range of U, with the CDW order parameter approaching zero asymptotically for large U. In the large U regime, the system behaves as a MI with AF

order. For weak to intermediate Δ, decreasing the value of U, the system undergoes a transition to a correlated insulating phase suggesting bond order (BO) with a closing of the charge gap at the transition point $U_{c1}(\Delta)$. The transition also manifests itself via an abrupt increase in the slope of the staggered density, double occupancy, and staggered magnetization as a function of U. Further, the bond-ordered phase undergoes a first-order transition to a BI at a lower critical coupling $U_{c2}(\Delta)$ where the charge gap remains finite. AF order is found only in the MI and bond-ordered phases. For $\Delta \sim 4.5t$, the system undergoes a direct first-order transition from the BI to the MI, with a finite charge gap everywhere.

CDMFT is a nonperturbative technique where the full many-body problem is mapped onto local degrees of freedom treated exactly within a finite cluster that is embedded in a self-consistent bath. It is a natural generalization of single-site DMFT to incorporate spatial correlations. The method has passed rigorous tests for the 1D Hubbard model where it compares well to exact solutions [10]. CDMFT has also been used to elucidate various aspects of the phase diagram of the cuprates, including the pseudogap [11] and superconducting phases within the 2D Hubbard model [12].

Using CDMFT, the IHM on the infinite lattice in two dimensions reduces to the cluster-bath Hamiltonian below, which is subject to a self-consistency condition:

$$H = \sum_{\langle \mu\nu\rangle\sigma} t_{\mu\nu} c^{\dagger}_{\mu\sigma} c_{\nu\sigma} + U \sum_{\mu} n_{\mu\uparrow} n_{\mu\downarrow} + \Delta \sum_{\mu} (-1)^{\mu} n_{\mu} + \sum_{m\sigma} \epsilon_{m\sigma} a^{\dagger}_{m\sigma} a_{m\sigma} + \sum_{m\mu\sigma} V_{m\mu\sigma} (a^{\dagger}_{m\sigma} c_{\mu\sigma} + \text{H.c.}). \quad (2)$$

$\mu, \nu = 1, \ldots, N_c$ denote indices labeling the cluster sites and $m = 1, \ldots, N_b$ represent those in the bath. The self-consistent calculation proceeds by an initial guess for the cluster-bath hybridization $V_{m\mu\sigma}$ and the bath site energies $\epsilon_{m\sigma}$ to obtain the cluster Green function $G_c^{\mu\nu}$. Applying the Dyson equation, $\Sigma_c = G_{0c}^{-1} - G_c^{-1}$, where G_{0c} denotes the noninteracting Green function for the Hamiltonian in Eq. (2), the cluster self-energy is obtained. Σ_c is then used in the self-consistency condition below to determine a new G_{0c}:

$$G_{0c}^{-1}(z) - \Sigma_c(z) = \left[\frac{N_c}{4\pi^2} \int dK \frac{1}{z + \mu - t(K) - \Sigma_c(z)} \right]^{-1}. \quad (3)$$

Here, K denotes a momentum vector in the reduced Brillouin zone of the cluster superlattice and $z = i\omega_n$ is the fermionic Mastubara frequency. From G_{0c} in Eq. (3) a new set of $V_{m\mu\sigma}$ and $\epsilon_{m\sigma}$'s is generated closing an iterative loop. In this work, the Lanczos method is used to solve the cluster-bath Hamiltonian. The cluster size is fixed to $N_c = 4$ and the bath size to $N_b = 8$. The Lanczos method can access both the strong and weak coupling regimes with equal ease, and it is well suited to compute dynamical quantities directly in real frequency. Rotational symmetries of the cluster on a square lattice, together with particle-hole symmetry at half filling, reduce the number of bath parameters significantly. These bath parameters can depend on spin, allowing for symmetry breaking solutions. For details of the method, we refer to earlier work [9,10].

We analyze our results by starting with Fig. 1, which shows the density difference between sublattices A and B as a function of U, for $\Delta = 2t$. Clearly, the system presents long-range CDW order over the entire range of U. The CDW order parameter asymptotically approaches zero for increasing U but remains finite everywhere. Starting from the MI phase at large U, the staggered charge density increases smoothly as U is reduced, but at $U = U_{c1} = 5.4t$ there is an abrupt increase in the slope. This anomaly is clearly identified in the inset and it is believed to be a signature of the transition to a bond-ordered phase. This result is similar to observations in earlier DMRG calculations for the one-dimensional IHM [2,3]. The bond-ordered phase extends up to $U = U_{c2} = 4.6t$, where there is a first-order transition to a BI signaled by a jump in the staggered density. Starting from $U = 0$, the BI shows a continuous decrease in the staggered density and persists up to $U = 6.55t$. Consequently, we have the coexistence of a BI and a BO for $4.6t < U < 5.4t$ and a BI and a MI for $5.4t < U < 6.55t$. We computed the total energy in the coexistence region (not shown) and find that the BI solution for the CDMFT equations is always higher in energy than the BO or the MI phase for the same U.

To further characterize the nature of the transition let us consider the staggered magnetization, $M = n_{\uparrow} - n_{\downarrow}$, and the double occupancy, $D = \langle n_{\uparrow} n_{\downarrow} \rangle$, as a function of U for $\Delta = 2t$ shown in Fig. 2. With reducing U both these quantities show an abrupt increase in slope at the same transition point $U = U_{c1} = 5.4t$ (see insets) where the bond-ordered insulator emerges from the MI. Both M and D present a jump at the first-order transition from the bond-ordered phase to a BI. The staggered magnetization abruptly goes to zero upon entering the BI phase signifying an absence of AF order. The double occupancy

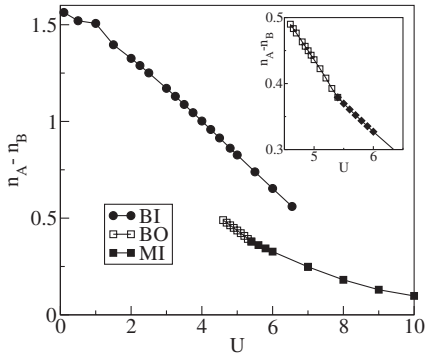

FIG. 1. Staggered charge density as a function of U in the BI, MI, and BO regions for $\Delta = 2t$. The inset shows an enlarged view of the abrupt change of slope at the MI-BO boundary.

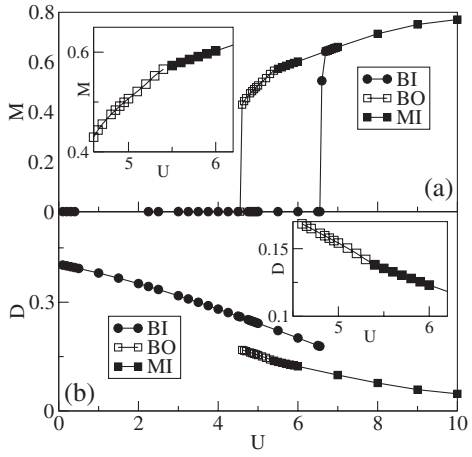

FIG. 2. (a) Staggered magnetization and (b) double occupancy as a function of U, for $\Delta = 2t$.

increases monotonically with reducing U in the BI state due to the increasing tendency towards CDW order.

In Fig. 3, results for the local density of states (LDOS) as a function of U for $\Delta = 2t$ are presented. Note that the LDOS shows particle-hole symmetry consistent with half filling because it is averaged over the A and B sublattices. For U equal to the bandwidth of $8t$, the spectra show lower and upper Hubbard bands consistent with a MI. In addition, sharp coherent peaks are observed (absent in single-site DMFT). They correspond to the motion of a carrier in an AF background and define the Mott gap. As U is lowered, the Mott gap reduces its value until it closes at the transition point $U = 5.4t$, which manifested itself earlier as an abrupt change in slope for the staggered density, double occupancy, and staggered magnetization. With further reduction in U, the trend for the Mott gap is reversed, with an increase in the gap in the bond-ordered phase. Further, at $U = 4.55$ there is an abrupt jump in the gap as compared to $U = 4.60$, signaling a transition to a BI, which also shows

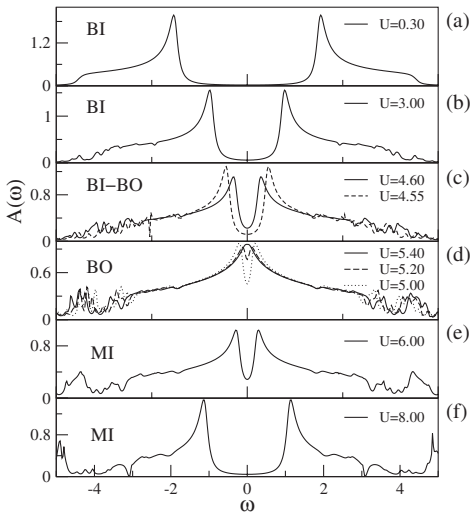

FIG. 3. Local density of states as a function of U for $\Delta = 2t$ shown with a broadening factor of $0.02t$.

an increasing gap with decreasing U. For $\Delta > 4.5t$, the BI-MI transition has no intervening phase and it is accompanied by the closing of the charge gap. This transition scenario is reminiscent of the phase diagram of the extended Hubbard model in one dimension, where an intermediate phase with bond order is stabilized between the CDW and spin-density wave phases only for intermediate strength of Coulomb repulsion U when the nearest-neighbor Coulomb repulsion V is varied [13].

To characterize the distinct phases observed, we have computed the momentum-dependent density of states using the following relation between the lattice Green function and the cluster self-energy:

$$G(\mathbf{k}, z) = \frac{1}{N_c} \sum_{\mu\nu} e^{i\mathbf{k}\cdot(\mu-\nu)} \left[\frac{1}{z + \mu - t(\mathbf{k}) - \Sigma(z)} \right]_{\mu\nu}. \quad (4)$$

In Fig. 4, we show the evolution of the density of states, $A(\mathbf{k}, \omega)$, in the first quadrant of the Brillouin zone, from $(0, 0)$ to (π, π). At large U [Fig. 4(c)] sharp coherent peaks that define the Mott gap are observed. In addition, the lower and upper Hubbard bands are present, as well as high energy features separated from them by Δ. The minimum of the gap is found at $\mathbf{k} = (\pi/2, \pi/2)$ where the low energy features disperse towards zero frequency, while the maximum of the gap is found at $\mathbf{k} = (\pi, \pi)$ or $(0, 0)$. For small U [Fig. 4(a)], where we have a BI, a dispersion characteristic of AF order is observed but with the notable absence of Hubbard bands. By contrast, for intermediate U, on the phase boundary of the MI-BO transition at $U = 5.4t$, we found a metallic density of states with distinct higher energy bands at $(\pi, 0)$ and $(0, \pi)$ that emerges from spontaneous dimerization and persists into the bond-ordered phase. Therefore, the bond-ordered phase, although similar to the BI in the behavior of the charge gap as a function of U, shows a distinct signature of strong

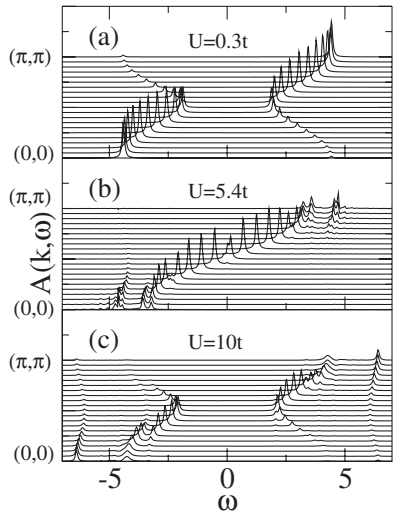

FIG. 4. Momentum-dependent density of states along the $(0, 0)$ to (π, π) direction for (a) the BI, (b) the phase boundary of the MI-BO transition, and (c) the MI for $\Delta = 2t$.

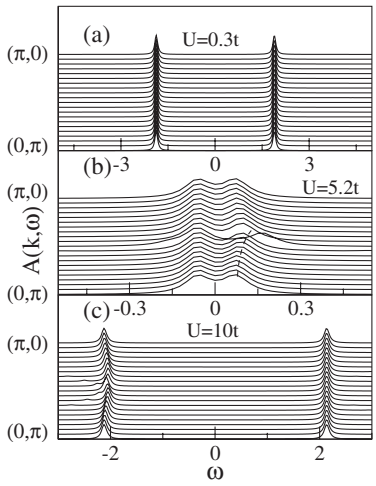

FIG. 5. Momentum-dependent density of states along the $(0, \pi)$ to $(\pi, 0)$ direction for $\Delta = 2t$.

correlations. The metallic peak itself splits to open a gap right below the phase boundary.

In Fig. 5, $A(\mathbf{k}, \omega)$ is shown, from $(0, \pi)$ to $(\pi, 0)$. The uncorrelated BI at $U = 0.3t$ [Fig. 5(a)] shows no dispersion of the low lying features and the gap becomes independent of momentum. For the MI phase at $U = 10t$ [Fig. 5(c)] we see an inward dispersion in the occupied band at $\mathbf{k} = (\pi/2, \pi/2)$ where the gap is a minimum, consistent with commensurate AF fluctuations. In contrast to this result, Fig. 5(b) for $U = 5.2t$ shows a maximum of the charge gap at $\mathbf{k} = (\pi/2, \pi/2)$ while the minimum lies at $\mathbf{k} = (0, \pi)$ or $(\pi, 0)$, consistent with the spontaneously dimerized bond-ordered phase with incommensurate order.

To summarize, we have studied the quantum phase transition between a BI and a MI in the two-dimensional IHM using CDMFT. CDW order persists throughout the entire range of U. For $\Delta < \Delta_c \sim 4.5t$, the large U Mott insulator state undergoes a transition to a correlated insulating phase BO with reducing U, accompanied by the closing of the charge gap at the transition point $U_{c1}(\Delta)$. The bond-ordered phase undergoes a first-order transition to a BI at $U_{c2}(\Delta)$ upon further reduction of U. As shown in the phase diagram depicted in Fig. 6, the width of the bond-ordered phase shrinks as both small and large Δ are approached. For $\Delta > \Delta_c$, a direct first-order MI-BI transition with no intervening bond-ordered phase is observed. AF order is found only in the MI and bond-ordered phases. Our results differ significantly from earlier ones that used the single-site DMFT technique [5] where a paramagnetic solution must be enforced even though the ground state is AF. Single-site DMFT misses spatial correlations crucial to the physics of this model. Moreover, the single-site DMFT finds a finite metallic region between the BI and the MI, whereas we find a single metallic point at the MI-BO ($\Delta < \Delta_c$) or MI-BI ($\Delta > \Delta_c$) transitions. Longer range interactions could give rise to a metallic phase between the insulators [14]. Our results are fairly similar to those obtained for this model using DMRG [2,3] in one dimension. An important difference is that at the metallic point we observe a closing of the charge gap, whereas DMRG finds only a closing of the optical gap, with the charge gap remaining finite over the entire range of U. The two-transition scenario moving from the BI to the MI was observed earlier in the weak coupling regime using Bosonization [4] for this model in one dimension. We have shown that a similar transition persists in two dimensions, even in the strong coupling regime when Δ is comparable to half the bandwidth. Modulation of the local potential with an alternating value could be realized in a two-dimensional optical lattice loaded with ultracold Fermionic atoms. Noise correlations in time-of-flight images can be used to distinguish between the AF, BI, and bond-ordered phases [15]. Energy gaps can be obtained, in principle, using rf spectroscopy [16]. We expect our results, predicting a novel correlated insulating phase with bond order, to motivate such experiments to verify our finding.

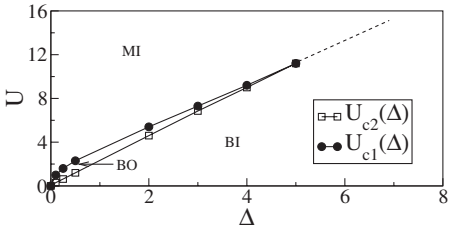

FIG. 6. Proposed CDMFT phase diagram for the 2D IHM.

S. S. K. is supported by the LDRD program at Oak Ridge National Laboratory. E. D. acknowledges support by NSF Grant No. DMR-0454504.

[1] C. D. Batista and A. A. Aligia, Phys. Rev. Lett. **92**, 246405 (2004).
[2] S. R. Manmana *et al.*, Phys. Rev. B **70**, 155115 (2004).
[3] A. P. Kampf *et al.*, J. Phys. Condens. Matter **15**, 5895 (2003).
[4] M. Fabrizio, A. O. Gogolin, and A. A. Nersesyan, Phys. Rev. Lett. **83**, 2014 (1999).
[5] A. Garg, H. R. Krishnamurthy, and M. Randeria, Phys. Rev. Lett. **97**, 046403 (2006).
[6] J. Hubbard and J. B. Torrance, Phys. Rev. Lett. **47**, 1750 (1981).
[7] T. Egami *et al.*, Science **261**, 1307 (1993).
[8] Z. Hadzibabic *et al.*, Phys. Rev. Lett. **91**, 160401 (2003).
[9] G. Kotliar *et al.*, Phys. Rev. Lett. **87**, 186401 (2001).
[10] C. J. Bolech, S. S. Kancharla, and G. Kotliar, Phys. Rev. B **67**, 075110 (2003); M. Capone, M. Civelli, S. S. Kancharla, C. Castellani, and G. Kotliar, Phys. Rev. B **69**, 195105 (2004).
[11] B. Kyung *et al.*, Phys. Rev. B **73**, 165114 (2006).
[12] S. S. Kancharla *et al.*, cond-mat/0508205.
[13] M. Nakamura, Phys. Rev. B **61**, 16 377 (2000).
[14] D. Poilblanc *et al.*, Phys. Rev. B **56**, R1645 (1997).
[15] M. Greiner *et al.*, Phys. Rev. Lett. **94**, 110401 (2005).
[16] C. Chin *et al.*, Science **305**, 1128 (2004).